Published in final edited form as:
Int J Radiat Oncol Biol Phys. 2010 November 1; 78(3): 743–750. doi:10.1016/j.ijrobp.2009.08.040.

Predicting Post-External-beam Radiation Therapy PSA Relapse of Prostate Cancer Using Pre-treatment MRI

Michael H. Fuchsjäger, MD[1,*], **Darko Pucar, MD, PhD**[1,*], **Michael J Zelefsky, MD**[2], **Zhigang Zhang, PhD**[3], **Qianxing Mo, PhD**[3], **Leah S. Ben-Porat, MS**[3], **Amita Shukla-Dave, PhD**[1,4], **Liang Wang, MD, PhD**[1], **Victor E. Reuter, MD**[5], and **Hedvig Hricak, MD, PhD**[1]

[1]Department of Radiology, Memorial Sloan-Kettering Cancer Center, New York

[2]Department of Radiation Oncology, Memorial Sloan-Kettering Cancer Center, New York

[3]Department of Epidemiology-Biostatistics, Memorial Sloan-Kettering Cancer Center, New York

[4]Department of Medical Physics, Memorial Sloan-Kettering Cancer Center, New York

[5]Department of Pathology, Memorial Sloan-Kettering Cancer Center, New York

Abstract

Purpose—To investigate whether pre-treatment endorectal magnetic resonance imaging (MRI) findings can predict biochemical relapse in patients with clinically localized prostate cancer (PCa) treated with external-beam radiation therapy (EBRT).

Patients and Methods—Between January 2000 and January 2002, 224 patients (median age 69 years, range 45-82) with biopsy-proven PCa underwent endorectal MRI before high-dose (≥ 81 Gy) EBRT. The value of multiple clinical and MRI variables in predicting PSA relapse at 5 years was determined using univariate and multivariate stepwise Cox regression. Clinical variables included pre-treatment PSA, clinical T-stage, Gleason score, use of neoadjuvant hormonal therapy and radiation dose. MRI variables, derived from retrospective consensus readings by two radiologists, measured intraprostatic and extraprostatic tumor burden.

Results—After median follow-up of 67 months, 37 patients (16.5%) developed PSA relapse. The significant predictors of PSA relapse in univariate analysis were pre-treatment PSA, clinical T-stage, and multiple MRI variables including MRI TN-stage score; extracapsular extension (ECE) status; number of sextants involved by ECE, all lesions, or index (dominant) lesion; apical involvement; and diameter and volume of index lesion. Pretreatment PSA and ECE status were the only significant independent predictors upon multivariate analysis ($P < 0.05$ for both). ECE status was associated with the highest hazard ratio of 3.04; 5-year PSA relapse rates were 7% for no ECE, 20% for unilateral ECE, and 48% for bilateral ECE.

Conclusion—MRI findings can be used to predict post-EBRT PSA relapse, with ECE status on MRI and pre-treatment PSA being significant independent predictors of this endpoint.

Corresponding author: Hedvig Hricak, MD, PhD Chairman, Dept. of Radiology Memorial Sloan-Kettering Cancer Center 1275 York Avenue New York, New York 10065 Tel: (212) 639-7475 Fax: (212) 794-4010 hricakh@mskcc.org.
*M.H. Fuchsjäger and D. Pucar contributed equally to this work.

Conflicts of Interest Notification
No conflicts of interest exist.

Keywords

MR imaging; prostate cancer; external beam radiation therapy; biochemical recurrence; extracapsular extension

Introduction

Numerous treatment options are available for patients with newly diagnosed prostate cancer, including radical prostatectomy (RP), external-beam radiation therapy (EBRT), brachytherapy, experimental focal therapies, and active surveillance. Predictions of their respective outcomes based on known prognostic factors can help the clinician and the patient choose among them. Because no single clinical predictor is sufficiently accurate for outcome prediction, nomograms have been developed that combine multiple predictors (1-5). The pre-treatment variables typically included in the nomograms are serum PSA, clinical T-stage and Gleason score; post-radiation therapy nomograms have included the use of neoadjuvant hormonal therapy and radiation dose.

Although current prognostic models for prostate cancer are reasonably accurate, there is an ongoing effort to improve their accuracy by including additional clinical and imaging variables (6-13). With its excellent soft-tissue resolution, endorectal magnetic resonance imaging (MRI) of the prostate clearly depicts the prostate's zonal anatomy and facilitates prostate cancer localization and staging (14-19). MRI has been shown to contribute significant incremental value to clinical variables in the prediction of extracapsular extension (ECE) and seminal vesicle invasion (SVI) and to significantly improve treatment planning (20-24). A number of studies have assessed the feasibility of MRI-inclusive models for predicting the outcome of radical prostatectomy or radiation therapy in patients with prostate cancer (7,9-11,25). In all of these studies, locally advanced prostate cancer on MRI (≥T3 disease) was associated with adverse outcomes, and in most it proved to be a significant independent predictor of treatment failure (7,9-11,25). The purpose of our study was to further investigate whether pre-treatment endorectal MRI findings can predict biochemical relapse in patients with clinically localized prostate cancer treated with EBRT.

PATIENTS AND METHODS

Patient Population

Our institutional review board approved and issued a waiver of informed consent for our retrospective review of the data of 224 consecutive patients (median age 69 years, range 45–82) with biopsy-proven prostate cancer who underwent endorectal MRI before EBRT between January 2000 and January 2002. Our study was compliant with the Health Insurance Portability and Accountability Act.

Acquisition and interpretation of clinical predictors

The clinical predictors recorded were pretreatment PSA, clinical stage, Gleason score, use of neoadjuvant hormone therapy, and radiation dose.

Pretreatment PSA was measured in ng/mL using either Tosoh (Tosoh USA, Inc., Grove City, OH) or Bayer (Immuno 1) assays (Siemens Healthcare Diagnostics, Deerfield, IL). For each patient, pretreatment clinical stage was assigned by a radiation oncologist according to the 1997 International Union against Cancer (IUCC) TNM staging system. Pre-treatment Gleason score was based on sextant biopsy results.

Neoadjuvant androgen deprivation therapy (ADT) was given to 121 (54%) patients before EBRT. In general patients were treated with 3-6 months of ADT before and concurrent with radiotherapy. ADT was given to decrease the size of enlarged prostate glands before radiotherapy or for those with high-grade, unfavourable-risk disease. ADT was routinely discontinued at the completion of radiotherapy. In high-risk patients within this radiotherapy cohort, adjuvant ADT was not used.

Patients received a dose of either 8100 cGy (n=125, 55.8%) or 8640 cGy (n=99, 44.2%). Treatment was delivered with 15MVx-rays in daily fractions of 1.8 Gy. All patients were treated with a five- or six-field conformal treatment approach as previously described (26). Doses were prescribed to the maximum isodose line, which completely encompassed the planning target volume. The planning target volume was defined as the prostate and seminal vesicles with a circumferential 1-cm margin except at the prostate-rectal interface, where a 6-mm margin was used. The techniques for treatment planning and delivery of three-dimensional conformal radiation therapy and intensity-modulated radiation therapy (IMRT) have been described elsewhere (26).

Acquisition and interpretation of endorectal MR predictors

Pre-treatment endorectal MRI was performed on a 1.5-Tesla whole-body magnetic resonance scanner (Signa Horizon scanner, General Electric Medical Systems, Milwaukee, WI) using a standard, previously described protocol (20). The median interval between MRI and EBRT was 3 months (range, 0-14 months). The longer interval in some patients was related to the use of neoadjuvant androgen deprivation therapy for decreasing prostatic size which extended in some cases to 10-12 months prior to initiation of radiotherapy.

Endorectal MRI studies were retrospectively interpreted in consensus by two radiologists (-- with 5 years of experience and -- with one and a half years of experience in dedicated reading of prostate MRI), with the senior reader prevailing if in dissent. The readers were aware that all patients had been diagnosed with prostate cancer and treated with EBRT but were unaware of any other clinical or outcome data. A picture archiving and communications system (PACS, Centricity 2.1 Radiology RA 1000, General Electric Medical Systems, Milwaukee, WI) and its built-in tools were used for qualitative image interpretation and quantitative measurements. Three distinct categories of MRI variables were determined, as described below.

Category 1) MRI staging variables: MRI TN stage score, number of prostate sextants with ECE, ECE status, SVI status, and lymph node invasion (LNI) status were recorded. For MRI-TN stage, the readers used an 8-point scoring system (developed in consensus by the institution's prostate cancer disease management team) following the 1992 International Union Against Cancer TNM staging system: 1, no tumor seen (corresponding to T1c); 2, tumor involves one-half of one lobe or less, no ECE (T2a); 3, tumor involves more than one-half of one lobe, no ECE (T2b); 4, tumor involves both lobes, no ECE (T2c); 5, unilateral ECE (T3a); 6, bilateral ECE (T3b); 7, SVI (T3c); 8, tumor invades adjacent structures other than seminal vesicles and/or lymph node metastasis (LNM) (T4 and/or N1). When multiple positive findings on endorectal MRI were seen, the highest applicable score was assigned. The number of prostate sextants with ECE was recorded. Scores were assigned for ECE status (0, no ECE; 1, unilateral ECE; 2, bilateral ECE), SVI status (0, no SVI; 1, unilateral SVI; 2, bilateral SVI) and LNI status (0, no LNI; 1, LNI).

Category 2) MRI variables based on all lesions observed: The number of sextants involved by all lesions (0-6) and the absence or presence of lesion(s) in the base, mid gland and apical sextants were recorded.

Category 3) MRI variables based on individual lesions: The number (0-6) of sextants involved by the index (dominant) lesion and the absence or presence of the index lesion in the base, mid gland and apical sextants; the maximal diameter and the volume of the index lesion; and the absence or presence of a second lesion > 10 mm were recorded.

Post-treatment patient follow-up

Patients were followed every six months after completion of EBRT with serial PSA testing and rectal examination. After five years, patients were followed annually. PSA relapse was defined as a post-EBRT serum PSA level 2 ng/mL or more above the nadir level consistent with the Phoenix definition of biochemical relapse after radiotherapy (27).

Statistical analysis

PSA relapse was used as a patient outcome measure. For statistical analysis, clinical T-stage and Gleason score were expressed as ordinally ranked discrete variables; use of neoadjuvant hormonal therapy and radiation dose were expressed as dichotomous variables; pretreatment PSA was expressed as a continuous variable (Table 1). Table 2 specifies which MRI variables were expressed as ordinally ranked discrete variables and which were expressed as dichotomous or continuous variables upon statistical analysis.

Nonparametric log-rank tests were used first as univariate analyses to illustrate differences among various levels of a predictor without taking into account other predictors. To quantify the differences and to incorporate multiple predictors, semiparametric Cox models were then fitted both univariately and multivariately to obtain hazard ratios. Using the stepwise selection procedure a multivariate Cox model was constructed, in which an effort was made to find an optimal subset by adding variables into the model or removing variables from the model one at a time. Variables were added to the model if the score Chi-Square statistic achieved a p-value of 0.05 or less, and removed from the model if the Wald Chi-Square statistic achieved a p-value of 0.05 or greater.

Descriptive statistics of mean and range were used to summarize the patient cohort with respect to clinical, MR imaging, and outcome variables. The Kaplan-Meier plots were used to illustrate the relationships between the selected pre-treatment clinical and MRI predictors and the post-RT PSA relapse. The significance levels of the differences among various Kaplan-Meier actuarial survival estimates for freedom from PSA relapse were determined using the log-rank test. Where applicable, a priori cut-offs based on the published studies were set to stratify the variables into 3 discrete levels for Kaplan-Meier plots.

P-values and 95% confidence intervals are two-sided. A p-value less than 0.05 was considered statistically significant. SAS 9.1.3 (SAS institute Inc., Cary, NC) and R 2.6.0 were used for the analysis.

RESULTS

As of January 2008, 37 (16.5%) of the 224 patients in this study had experienced PSA relapse. The median follow-up period was 67 months for all patients, 64 months for patients with no PSA relapse and 78 months for those with PSA relapse.

In the univariate Cox regression analysis, the statistically significant clinical predictors of PSA relapse were pre-treatment PSA and clinical T-stage (Table 1). Among the MRI parameters, the significant predictors in category 1 were MRI TN stage, ECE status and number of sextants with ECE; the significant predictors in category 2 were number of sextants involved by all lesions and the presence of tumor in the apex of the gland; the significant predictors in category 3 were the number of sextants involved by the index lesion, the index lesion diameter and the

index lesion volume (Table 2). The distribution of clinical and selected MRI findings among the patients and the probability of PSA relapse associated with each finding were tabulated (Tables 3 and 4).

In the multivariate Cox regression analysis, the only significant predictors of PSA relapse were pre-treatment PSA (hazard ratio, 1.02 [95% CI: 1.01 – 1.03]; p=0.0004) and ECE status on MRI (hazard ratio, 3.04 [95% CI: 1.93 – 4.80]; p<0.0001).

Kaplan-Meier estimates of PSA relapse-free survival for pre-treatment PSA, MRI TN stage, ECE status on MRI, and index lesion volume are illustrated in Figure 1. Figure 2 shows T2-weighted MR images from 4 representative cases.

DISCUSSION

Knowledge of the likelihood of biochemical recurrence or metastatic progression of prostate cancer is essential for rational treatment selection. In our retrospective study, with a patient population of 224 and a median follow up of 67 months, the status of ECE on MRI was a significant predictor of post-EBRT PSA relapse.

A number of clinical and pathological findings have been reported to be associated with the risk of recurrence. Despite its limited specificity for prostate cancer detection, the PSA level remains a powerful prognostic factor in the prediction of patient outcomes (25,28,29). Similarly, high Gleason score on sextant biopsy (8-10) and advanced clinical T-stage on digital rectal exam (T3a) have been associated with adverse outcomes (30). However, because none of these clinical variables alone is sufficient to accurately predict outcome and guide treatment selection, nomograms that combine multiple variables have been developed (1,5,31). A recent version of a nomogram for post-EBRT outcome prediction combined pre-treatment PSA, clinical T-stage, Gleason score, use (or lack) of neoadjuvant androgen deprivation therapy, and radiation dose to predict PSA-relapse in 2253 patients with a median follow-up of 7 years and achieved a concordance index of 0.72 (5).

A number of studies have investigated the utility of dedicated prostate MRI findings for predicting primary prostate cancer treatment outcomes (6,7,9-11). A retrospective study of 977 RP-treated men with 2-year follow-up for PSA relapse found preoperative PSA, percentage of positive prostate biopsies, endorectal MRI T-stage, biopsy Gleason score and clinical stage T2c disease to be independent predictors of PSA relapse (7). Another study by the same group in 1025 men treated with RP showed that MRI contributed incremental prognostic value to clinical parameters in about 20% of patients, specifically those patients considered to be at intermediate risk of PSA failure based on established clinical prognostic factors; when MRI was interpreted as indicating extracapsular versus organ-confined disease in these patients, the relative risk of PSA failure was 3.6, and 5-year actuarial freedom from PSA failure was 33% versus 72% (6).

Retrospective studies have shown MRI T-stage to have incremental value in predicting post-EBRT outcomes as well, though in smaller data sets (9-11). In a study of 250 patients with a median follow up of 28 months, MRI findings of SVI had independent prognostic value; 4-year estimates of PSA failure-free survival for MRI SVI-negative and MRI SVI-positive patients were 68% and 33%, respectively (11). Two recent studies by one research group showed that the predictive value of an individual MRI predictor could be influenced by other predictors in the set (9,10). In the first study 80 patients had mean post-EBRT follow-up of 43 months, and clinical parameters as well as the MRI tumor stage and the radial diameter of ECE on MRI were used as predictors; the only independent predictor of metastatic relapse in multivariate analysis was the radial diameter of ECE on MRI (10). In the second study 67 patients had mean post-EBRT follow-up of 44 months, and the volume of abnormal metabolism

on MR spectroscopic imaging and multiple MRI predictors were added to the model; the only independent predictor of PSA relapse was the volume of malignant metabolism on MR spectroscopic imaging, while the independent predictors of metastatic failure were MRI tumor size and SVI on MRI (9).

We found that pre-treatment PSA and ECE status on MRI were the only two significant independent predictors of PSA relapse after EBRT in the Cox model. Our results are in agreement with those of prior MRI-inclusive studies in patients treated with EBRT or RP: Although the designs of the studies varied, T3 disease on MRI was universally associated with adverse post-treatment outcomes (6,7,9-11). Larger, multi-institutional trials are needed to determine whether the status of ECE on MRI (no ECE, unilateral ECE, or bilateral ECE) is consistently the strongest independent MR imaging predictor of biochemical recurrence and a direct reflection of radiocurability.

In the MR imaging TN-stage scoring system used in our study, a higher score was assigned for each increase in stage. Higher pathologic stages are associated with higher rates of biochemical recurrence (32,33), and the capacity to successfully identify key features of pathologic stage (i.e., ECE, SVI and LNM) on MRI has been demonstrated (20,22-24,32). In our study, stratification of patients into three groups according to MRI TN-stage (Fig. 1B) was highly predictive of biochemical recurrence of prostate cancer after radiotherapy.

As new systemic approaches are being developed to treat patients with high-risk prostate cancer, it is becoming increasingly important to distinguish the subset of patients who may benefit from these systemic treatments from those who are unlikely to benefit and who can therefore be spared from their additional toxicity. Our data could be used in the future to stratify patients into risk groups (i.e. low, intermediate, high) for different treatment options such as neoadjuvant chemotherapy, neoadjuvant hormone therapy or immunotherapy (34).

The present study has several limitations, including its retrospective nature and the fact that it was performed at a single institution. MR imaging was performed with standard sequences and without a contrast agent. Diffusion-weighted imaging is now used routinely at our institution in prostate MR imaging and has been found to aid in cancer detection and assessment of tumor volume in the prostate (35,36). MR spectroscopic imaging and dynamic contrast-enhanced imaging may also improve prostate cancer detection and staging, particularly for less experienced readers (18,37-40). However, in 2000, when the MR images used in this study began to be collected, such advanced MR imaging techniques were not part of our routine imaging protocols.

Another possible limitation of our study is the relatively wide range of the intervals between MR imaging and the start of EBRT (6-415 days). However, the median interval was only 85 days. The longer interval time periods between MRI and initiation of EBRT reflect in general patients who were treated with neoadjuvant androgen deprivation therapy (ADT) where prostate volume reduction was required prior to the initiation of radiotherapy. In some cases maximal volume reduction was only achieved after 9-10 months before the radiotherapy was initiated. It should also be noted that the two radiologists who retrospectively interpreted the MR images for our study had experience reading prostate MR imaging at an institution where it is routinely performed. Therefore, the results may only represent the performance of this technique at institutions where prostate MRI is used routinely and will need to be validated in other academic and community settings.

At present, prostate MRI is a technically and interpretatively challenging modality used primarily at academic centers, and thus its nationwide use for prostate cancer prognostication cannot be recommended. To date, all MRI-inclusive studies on outcome prediction in patients with prostate cancer have been retrospective and have been based on small sample sizes. Yet

even if a prospective multi-institutional MRI prediction study is initiated, it will probably require a minimum of a decade to complete. We believe that the presently available evidence warrants the use of MRI findings to identify high-risk patients at centers where prostate MRI is routinely performed. Among patients with MRI evidence of extraprostatic disease, particularly bilateral ECE and/or SVI, more intensive treatment regimens may be warranted to achieve superior disease control outcomes. These regimens could include longer courses of androgen deprivation therapy, as well as more intensive dose escalation regimens which can be achieved with the combination of brachytherapy and IMRT.

Acknowledgments

This research was supported by National Institutes of Health grant #R01 CA76423. Dr. Fuchsjäger was supported by a stipend from the Max Kade Foundation, New York.

The authors thank Ada Muellner, BA, for editing the manuscript.

REFERENCES

1. Kattan MW, Eastham JA, Stapleton AM, et al. A preoperative nomogram for disease recurrence following radical prostatectomy for prostate cancer. J Natl Cancer Inst 1998;90:766–771. [PubMed: 9605647]
2. Kattan MW, Zelefsky MJ, Kupelian PA, et al. Pretreatment nomogram for predicting the outcome of three-dimensional conformal radiotherapy in prostate cancer. J Clin Oncol 2000;18:3352–3359. [PubMed: 11013275]
3. Ross RW, Kantoff PW. Predicting outcomes in prostate cancer: how many more nomograms do we need? J Clin Oncol 2007;25:3563–3564. [PubMed: 17704399]
4. Stephenson AJ, Scardino PT, Eastham JA, et al. Preoperative nomogram predicting the 10-year probability of prostate cancer recurrence after radical prostatectomy. J Natl Cancer Inst 2006;98:715–717. [PubMed: 16705126]
5. Zelefsky MJ, Kattan MW, Fearn P, et al. Pretreatment nomogram predicting ten-year biochemical outcome of three-dimensional conformal radiotherapy and intensity-modulated radiotherapy for prostate cancer. Urology 2007;70:283–287. [PubMed: 17826490]
6. D'Amico AV, Whittington R, Malkowicz B, et al. Endorectal magnetic resonance imaging as a predictor of biochemical outcome after radical prostatectomy in men with clinically localized prostate cancer. J Urol 2000;164:759–763. [PubMed: 10953141]
7. D'Amico AV, Whittington R, Malkowicz SB, et al. Combination of the preoperative PSA level, biopsy gleason score, percentage of positive biopsies, and MRI T-stage to predict early PSA failure in men with clinically localized prostate cancer. Urology 2000;55:572–577. [PubMed: 10736506]
8. Fuchsjäger MH, Shukla-Dave A, Hricak H, et al. MR imaging in the prediction of biochemical recurrence of prostate cancer after radical prostatectomy. BJU Int. 2009 [Epub ahead of print].
9. Joseph T, McKenna DA, Westphalen AC, et al. Pretreatment Endorectal Magnetic Resonance Imaging and Magnetic Resonance Spectroscopic Imaging Features of Prostate Cancer as Predictors of Response to External Beam Radiotherapy. Int J Radiat Oncol Biol Phys 2009;73:665–671. [PubMed: 18760545]
10. McKenna DA, Coakley FV, Westphalen AC, et al. Prostate cancer: role of pretreatment MR in predicting outcome after external-beam radiation therapy--initial experience. Radiology 2008;247:141–146. [PubMed: 18258811]
11. Nguyen PL, Whittington R, Koo S, et al. Quantifying the impact of seminal vesicle invasion identified using endorectal magnetic resonance imaging on PSA outcome after radiation therapy for patients with clinically localized prostate cancer. Int J Radiat Oncol Biol Phys 2004;59:400–405. [PubMed: 15145155]
12. Pucar D, Koutcher JA, Shah A, et al. Preliminary assessment of magnetic resonance spectroscopic imaging in predicting treatment outcome in patients with prostate cancer at high risk for relapse. Clin Prostate Cancer 2004;3:174–181. [PubMed: 15636684]

13. Shukla-Dave A, Hricak H, Kattan MW, et al. The utility of magnetic resonance imaging and spectroscopy for predicting insignificant prostate cancer: an initial analysis. BJU Int 2007;99:786–793. [PubMed: 17223922]

14. Bartolozzi C, Menchi I, Lencioni R, et al. Local staging of prostate carcinoma with endorectal coil MRI: correlation with whole-mount radical prostatectomy specimens. Eur Radiol 1996;6:339–345. [PubMed: 8798003]

15. Graser A, Heuck A, Sommer B, et al. Per-Sextant Localization and Staging of Prostate Cancer: Correlation of Imaging Findings with Whole-Mount Step Section Histopathology. AJR Am J Roentgenol 2007;188:84–90. [PubMed: 17179349]

16. Mullerad M, Hricak H, Kuroiwa K, et al. Comparison of endorectal magnetic resonance imaging, guided prostate biopsy and digital rectal examination in the preoperative anatomical localization of prostate cancer. J Urol 2005;174:2158–2163. [PubMed: 16280755]

17. Yu KK, Hricak H, Alagappan R, et al. Detection of extracapsular extension of prostate carcinoma with endorectal and phased-array coil MR imaging: multivariate feature analysis. Radiology 1997;202:697–702. [PubMed: 9051019]

18. Yu KK, Scheidler J, Hricak H, et al. Prostate cancer: prediction of extracapsular extension with endorectal MR imaging and three-dimensional proton MR spectroscopic imaging. Radiology 1999;213:481–488. [PubMed: 10551230]

19. Engelbrecht MR, Jager GJ, Laheij RJ, et al. Local staging of prostate cancer using magnetic resonance imaging: a meta-analysis. Eur Radiol 2002;12:2294–2302. [PubMed: 12195484]

20. Mullerad M, Hricak H, Wang L, et al. Prostate cancer: detection of extracapsular extension by genitourinary and general body radiologists at MR imaging. Radiology 2004;232:140–146. [PubMed: 15166319]

21. Sala E, Akin O, Moskowitz CS, et al. Endorectal MR imaging in the evaluation of seminal vesicle invasion: diagnostic accuracy and multivariate feature analysis. Radiology 2006;238:929–937. [PubMed: 16424250]

22. Wang L, Mullerad M, Chen HN, et al. Prostate cancer: incremental value of endorectal MR imaging findings for prediction of extracapsular extension. Radiology 2004;232:133–139. [PubMed: 15166321]

23. Wang L, Hricak H, Kattan MW, et al. Combined endorectal and phased-array MRI in the prediction of pelvic lymph node metastasis in prostate cancer. AJR Am J Roentgenol 2006;186:743–748. [PubMed: 16498101]

24. Wang L, Zhang J, Schwartz LH, et al. Prediction of seminal vesicle invasion in prostate cancer: incremental value of adding endorectal MR imaging to the Kattan nomogram. Radiology 2007;242:182–188. [PubMed: 17090712]

25. D'Amico AV, Whittington R, Malkowicz SB, et al. Utilizing predictions of early prostate-specific antigen failure to optimize patient selection for adjuvant systemic therapy trials. J Clin Oncol 2000;18:3240–3246. [PubMed: 10986056]

26. Burman C, Chui CS, Kutcher G, et al. Planning, delivery, and quality assurance of intensity-modulated radiotherapy using dynamic multileaf collimator: a strategy for large-scale implementation for the treatment of carcinoma of the prostate. Int J of Radiat Oncol Biol Phys 1997;39:863–873. [PubMed: 9369136]

27. Roach M 3rd, Hanks G, Thames H Jr, et al. Defining biochemical failure following radiotherapy with or without hormonal therapy in men with clinically localized prostate cancer: Recommendations of the RTOG-ASTRO Phoenix Consensus Conference. Int J Radiat Oncol Biol Phys 2006;65:965–974. [PubMed: 16798415]

28. Bauer JJ, Connelly RR, Sesterhenn IA, et al. Biostatistical modeling using traditional variables and genetic biomarkers for predicting the risk of prostate carcinoma recurrence after radical prostatectomy. Cancer 1997;79:952–962. [PubMed: 9041158]

29. Moul JW, Connelly RR, Lubeck DP, et al. Predicting risk of prostate specific antigen recurrence after radical prostatectomy with the Center for Prostate Disease Research and Cancer of the Prostate Strategic Urologic Research Endeavor databases. J Urol 2001;166:1322–1327. [PubMed: 11547066]

30. Freedland SJ, Humphreys EB, Mangold LA, et al. Risk of prostate cancer-specific mortality following biochemical recurrence after radical prostatectomy. JAMA 2005;294:433–439. [PubMed: 16046649]

31. Partin AW, Kattan MW, Subong EN, et al. Combination of prostate-specific antigen, clinical stage, and Gleason score to predict pathological stage of localized prostate cancer. A multi-institutional update. Jama 1997;277:1445–1451. [PubMed: 9145716]
32. Han M, Partin AW, Zahurak M, et al. Biochemical (prostate specific antigen) recurrence probability following radical prostatectomy for clinically localized prostate cancer. J Urol 2003;169:517–523. [PubMed: 12544300]
33. Hull GW, Rabbani F, Abbas F, et al. Cancer control with radical prostatectomy alone in 1,000 consecutive patients. J Urol 2002;167:528–534. [PubMed: 11792912]
34. Freedman GM, Negendank WG, Hudes GR, et al. Preliminary results of a bone marrow magnetic resonance imaging protocol for patients with high-risk prostate cancer. Urology 1999;54:118–123. [PubMed: 10414737]
35. Haider MA, van der Kwast TH, Tanguay J, et al. Combined T2-weighted and diffusion-weighted MRI for localization of prostate cancer. AJR Am J Roentgenol 2007;189:323–328. [PubMed: 17646457]
36. Mazaheri Y, Hricak H, Fine SW, et al. Prostate tumor volume measurement with combined T2-weighted imaging and diffusion-weighted MR: Correlation with pathologic tumor volume. Radiology. in press.
37. Bloch BN, Furman-Haran E, Helbich TH, et al. Prostate cancer: accurate determination of extracapsular extension with high-spatial-resolution dynamic contrast-enhanced and T2-weighted MR imaging - initial results. Radiology 2007;245:176–185. [PubMed: 17717328]
38. Fütterer JJ, Heijmink SW, Scheenen TW, et al. Prostate cancer localization with dynamic contrast-enhanced MR imaging and proton MR spectroscopic imaging. Radiology 2006;241:449–458. [PubMed: 16966484]
39. Fütterer JJ, Engelbrecht MR, Huisman HJ, et al. Staging prostate cancer with dynamic contrast-enhanced endorectal MR imaging prior to radical prostatectomy: experienced versus less experienced readers. Radiology 2005;237:541–549. [PubMed: 16244263]
40. Scheidler J, Hricak H, Vigneron DB, et al. Prostate cancer: localization with three-dimensional proton MR spectroscopic imaging – clinicopathologic study. Radiology 1999;213:473–480. [PubMed: 10551229]

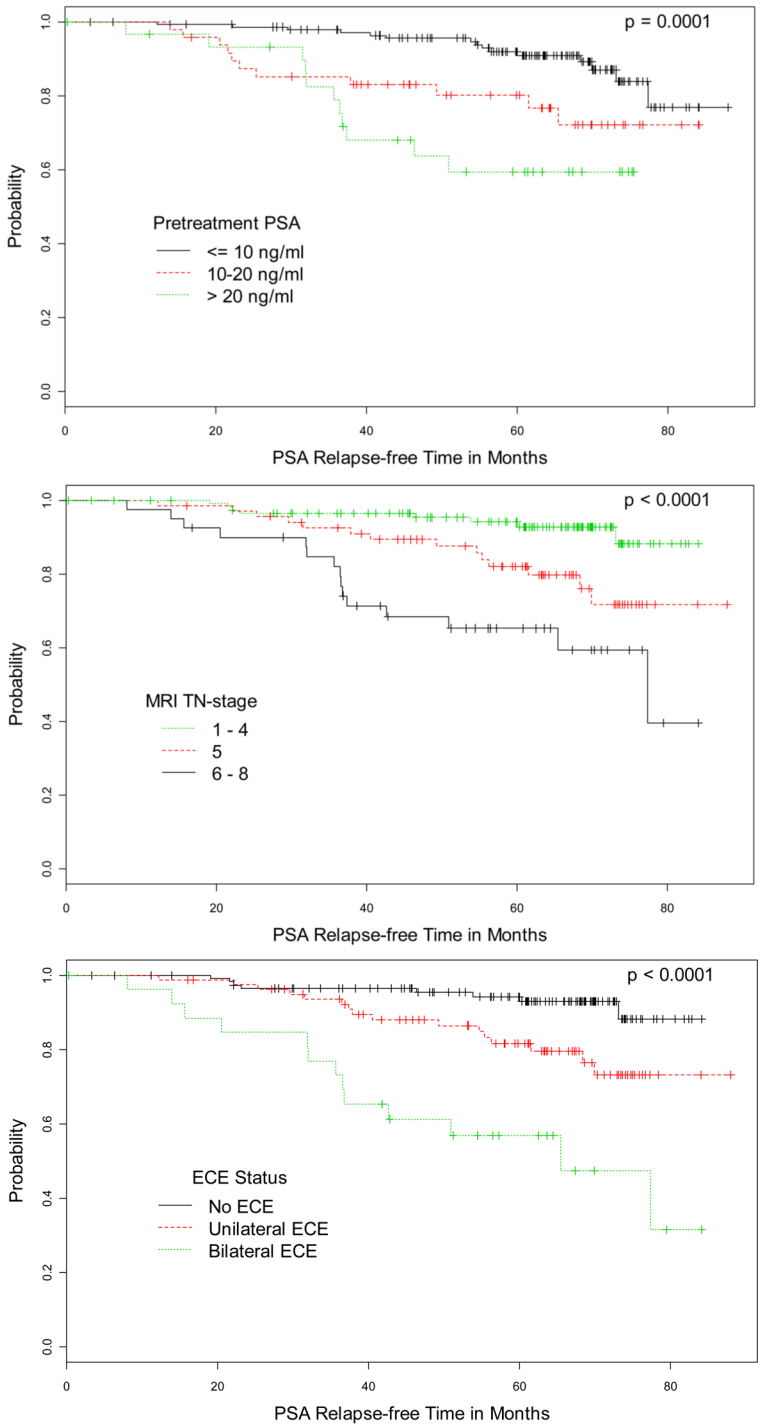

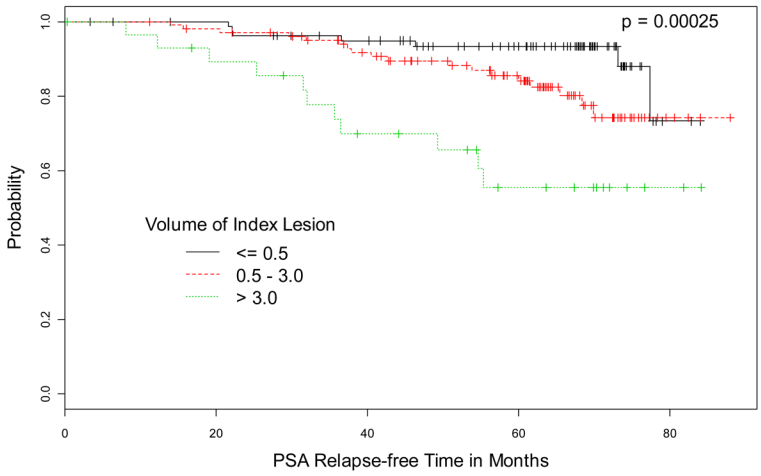

Figure 1.

Kaplan-Meier Estimates of PSA relapse-free survival based on (A) pre-treatment PSA, (B) MRI TN-stage score, (C) extracapsular extension (ECE) status on MRI, and (D) volume of index lesion. Graphs show cumulative proportions of patients without post-EBRT PSA relapse, stratified by PSA, MRI TN-stage score, ECE status on MRI, and volume of index lesion.

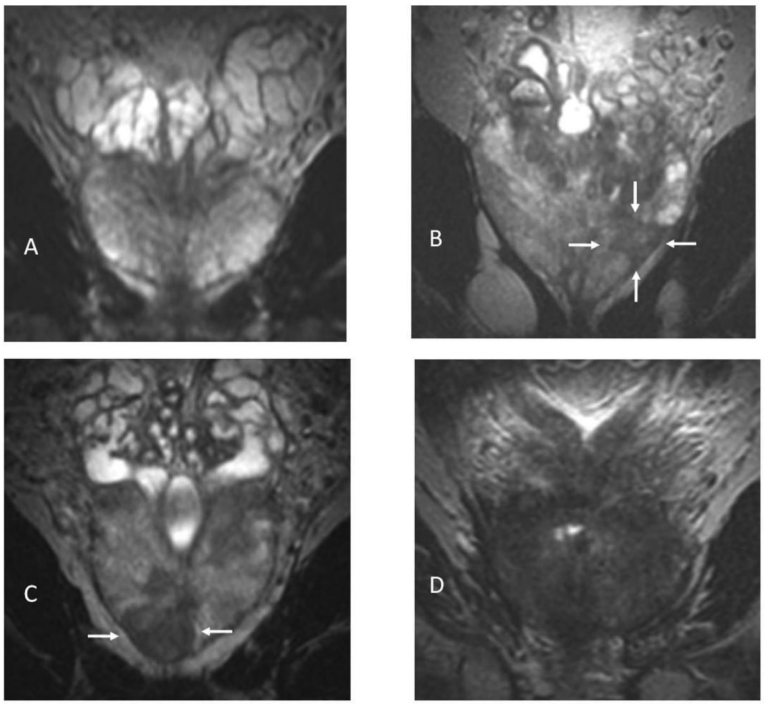

Figure 2.
Coronal T2-weighted MR images. Patients in A and B had neither extraprostatic disease nor PSA relapse, while patients in C and D had both. A) No lesion visible; B) 0.5-cm^3 lesion at left mid gland and apex (arrows). C) 1.7-cm^3 lesion in apex (arrows) with bilateral capsular irregularity and bulging indicating extracapsular extension (ECE). D), 11-cm^3 tumor with bilateral ECE and seminal vesicle invasion.

Table 1

Univariate Cox proportion hazards model for statistical significance of clinical predictors.

Variable	P-value	Hazard Ratio (95% CI)
Pre-treatment PSA†	<.001	1.02(1.01,1.03)
Clinical T-Stage*	0.03	1.23(1.02,1.48)
Gleason Score*	0.07	1.32(0.98,1.79)
Neoadjuvant Hormonal Therapy‡	0.19	1.58(0.80,3.10)
Radiation Dose‡	0.84	1.07(0.56,2.05)

*expressed as an ordinal variable;

†expressed as a continuous variable;

‡expressed as a dichotomous variable.

Table 2

Univariate Cox proportion hazards model for statistical significance of MRI predictors.

Variable	P-value	Hazard Ratio (95% CI)
MRI STAGING PARAMETERS		
MRI TN-Stage*	<.001	1.61(1.26,2.05)
ECE status*	<.001	3.04(1.96,4.71)
Number of sextants with ECE*	<.001	1.68(1.38,2.05)
SVI status*	0.14	1.88(0.82,4.33)
LNI status‡	0.45	0.58(0.14,2.41)
MRI PARAMETERS BASED ON ALL LESIONS OBSERVED		
Number of sextants involved by all lesions*	<.001	1.50(1.23,1.82)
Base sextants involved‡	0.19	1.58(0.80,3.15)
Mid gland sextants involved‡	0.99	n.a.
Apical sextants involved‡	0.03	2.41(1.10,5.28)
MRI PARAMETERS BASED ON INDIVIDUAL LESIONS		
Number of sextants involved by index lesion*	0.005	1.32(1.09,1.60)
Diameter of index lesion†	<.001	1.79(1.29,2.49)
Volume of index lesion†	<.001	1.17(1.08,1.27)
Base sextants involved by index lesion‡	0.16	1.60(0.84,3.04)
Mid gland sextants involved by index lesion‡	0.21	1.96(0.69,5.52)
Apical sextants involved by index lesion‡	0.06	1.88(0.97,3.62)
2nd lesion > 10 mm presence‡	0.37	1.46(0.64,3.33)

*expressed as an ordinal variable;

†expressed as a continuous variable;

‡expressed as a dichotomous variable.

Table 3

Distribution of cases (n=224) according to ranks or ranges for selected clinical predictors, with actual recorded events of PSA relapse for each rank or range.

Predictor	Distribution*		PSA relapse†	
PSA (ng/ml)				
0-5	63	(28.1)	4	(6.4)
5-10	82	(36.6)	11	(13.4)
10-15	31	(13.8)	7	(22.6)
15-20	17	(7.6)	4	(23.5)
> 20	31	(13.8)	11	(35.5)
Clinical T-stage				
cT1c	110	(49.1)	13	(11.8)
cT2a	66	(29.5)	12	(18.2)
cT2b	19	(8.5)	4	(21.0)
cT3a	17	(7.6)	5	(29.4)
cT3b	12	(5.4)	3	(25.0)
Gleason Score				
5	2	(0.9)	0	(0)
6	101	(45.1)	11	(10.9)
7	78	(34.8)	14	(17.6)
8	29	(13.0)	11	(37.9)
9	13	(5.8)	1	(7.7)
10	1	(0.4)	0	(0)
Neoadjuvant hormonal therapy				
No	103	(46.0)	13	(12.6)
Yes	121	(54.0)	24	(19.8)
Radiation dose				
8100 cGy	125	(55.8)	20	(16.0)
8640 cGy	99	(44.2)	17	(17.2)

Note.—Data are the number of patients.

*Number in parentheses represents percentage of total study population.

†Number in parentheses represents percentage of patients in the same row in the distribution column.

Table 4

Distribution of cases (n=224) according to ranks or ranges for selected MRI predictors, with actual recorded events of PSA relapse for each rank or range.

Predictor	Distribution*		PSA relapse†	
MRI TN-Stage Score				
1 (T1c)	1	(0.4)	0	(0)
2 (T2a)	23	(10.3)	1	(4.4)
3 (T2b)	37	(16.5)	3	(8.1)
4 (T2c)	55	(24.6)	4	(7.3)
5 (T3a, unilateral ECE)	68	(30.4)	14	(20.6)
6 (T3b, bilateral ECE)	22	(9.8)	11	(50.0)
7 (T3c, SVI)	16	(7.1)	4	(25.0)
8 (T4 or N1)	2	(0.9)	0	(0)
ECE status				
0 (no ECE)	117	(52.2)	8	(6.8)
1 (unilateral ECE)	80	(35.7)	16	(20.0)
2 (bilateral ECE)	27	(12.0)	13	(48.2)
Number of sextants with ECE				
0	117	(52.2)	8	(6.8)
1	47	(20.9)	7	(14.9)
2	37	(16.5)	13	(35.1)
3	14	(6.2)	5	(35.7)
4	8	(3.6)	4	(50.0)
5	0	(0)	0	(0)
6	1	(0.4)	0	(0)
Number of sextants involved by all				
0	1	(0.4)	0	(0)
1	40	(17.9)	2	(5.0)
2	64	(28.6)	6	(9.4)
3	40	(17.9)	4	(10.0)
4	33	(14.7)	11	(33.3)
5	15	(6.7)	3	(20.0)
6	31	(13.8)	11	(35.5)
Volume of index				
< 0.5	93	(38.5)	8	(8.6)
0.5-1.0	40	(18.8)	8	(20.0)
1.0-2.0	50	(23.5)	6	(12.0)

Predictor	Distribution*		PSA relapse†	
2.0-3.0	12	(5.6)	4	(33.3)
> 3	29	(13.6)	11	(37.9)

Note.—Data are the number of patients.

*Number in parentheses represents percentage of total study population.

†Number in parentheses represents percentage of patients in the same row in the distribution column.